Egypt. J. Chem. **Vol.** 68, SI: Z. M. Nofal, pp. 1099- 1110(2025)

Egyptian Journal of Chemistry

http://ejchem.journals.ekb.eg/

Electrochemically Synthesized Molecularly Imprinted Polymers for Potentiometric Sensing of Manganese (II) in Petroleum Wastewater

Hoyeda Elsayaed Ibrahim[1], Ahmed Othman Mahmoud[1], Salah Mahmoud Rashwan[1], Tamer Awad Ali *[2]

[1]*Chemistry Department, Faculty of Science, Suez Canal University,Egypt*

[2] *Egyptian Petroleum Research Institute (EPRI), 11727 Cairo, Egypt*

Abstract

The synthesis of a manganese ion-imprinted polymer was carried out using thermal polymerization. This process involved methacrylic acid as the functional monomer, ethylene glycol dimethacrylate (EGDMA) as the cross-linking agent, ammonium persulfate as the polymerization initiator, dithizone as the manganese-binding ligand, and manganese ions as the template ion. Ethanol served as the reaction medium to facilitate the polymerization process. Following the synthesis, an electrochemical sensor was developed, designed specifically for the determination of manganese (II) ions with high selectivity. This sensor utilized a modified carbon paste electrode (MCPE), which was further enhanced by the incorporation of multi-walled carbon nanotubes (MWCNTs). The inclusion of MWCNTs significantly improved the performance characteristics of the electrode by increasing its conductivity and surface area. They found linear concentration ranges of 1.0 × 10-7 to 1.0×10-1 mol L-1, with Nernstian slopes of 29.74 ± 0.18 mV decade-1. The detection limit for the carbon paste electrode (Electrode III) was 1.0 × 10-7 mol L-1, and the electrode (III) response time was 8 s. Without a divergence, the paste may be used for more than 125 days, and the electrode (III) can detect pH levels ranging from 3.5 to 8.5. Electrode (III) has an isotherm coefficient of 0.00016 V/ºC. The interference effects of other ionic species were thoroughly studied to assure selectivity, with findings validating the suggested electrode's capacity to discriminate manganese (II) ions from competing ions successfully. This underscores its applicability for practical applications requiring precision ion detection. The electrode architecture provides various benefits, including excellent sensitivity, selectivity, operating simplicity, and a very low detection limit. Furthermore, comparison studies were done to establish the performance of the electrochemical sensor versus atomic absorption spectrometry (AAS). These comparisons confirmed that the potentiometric sensor produces reliable and consistent results, establishing it as a competitive and efficient alternative for manganese (II) ion determination.

Keywords: Modified carbon paste electrode; Electrochemical sensor; Molecular imprinted polymer; Manganese (II) ion determination.

1. Introduction

Manganese is naturally present in many surface and groundwater sources, as well as in the soils that contribute to these water bodies through erosion. However, industrial activities can significantly increase manganese contamination in certain aquatic environments. The primary exposure pathways for the general public include the ingestion of manganese through both food consumption and drinking water [1].

Manganese is recognized as the third most abundant transition metal in the Earth's crust [2].

Manganese is extensively employed in numerous industrial applications such as steel production, alloys, varnishes, oils, disinfectants, batteries, paints, fertilizers, pesticides, ceramics, nutritional supplements, and recently, manganese-based nanoparticles for biomedical applications [3, 4].

Manganese is considered a micronutrient and an essential trace element for several bodily physiological processes, and inadequate absorption of this element may result in skeletal deficiency, impaired growth, impaired glucose tolerance, and reduced fertility [5, 6]. Conversely, high-level exposure to manganese, particularly within industrial environments, can result in its accumulation in the nervous system, leading to deleterious effects on human health. These adverse consequences include neurodegenerative conditions reminiscent of Parkinson's disease, as well as reproductive impairments such as sperm damage and diminished libido [7, 8].

As a result, tracking and determining the amount of manganese in environmental resources becomes crucial. X-ray fluorescence [9-11] Inductively coupled plasma atomic emission spectrometry (ICP-AES) [12, 13], spectrophotometry [14] Neutron activation analysis (NAA) [15, 16], and differential pulse anodic stripping voltammetry [17, 18] There are a few instrumental methods for determining manganese.

The development of manganese (II) ion determination methodologies that can be readily deployed across various industrial sectors is essential. Such techniques must be achievable with cost-effective, uncomplicated instrumentation while ensuring high accuracy and sensitivity in analytical measurements. Electrochemical methods address this need by utilizing electrodes that offer numerous advantages, including high sensitivity, low cost, rapid analysis times, and enhanced portability, especially when paired with modern, battery-operated, handheld potentiostat [19].

In this regard, electrochemical analysis has received increased attention because of its many advantages, including ease of use, affordability, speed, and the potential for downsizing [20-22]. Gaining sensors with desirable performance, excellent

*Corresponding author e-mail: dr_tamerawad@yahoo.com.; (Prof. Dr. Tamer Awad Ali).

Received date 04 May 2025; Revised date 03 June 2025; Accepted date 02 July 2025

DOI: 10.21608/ejchem.2025.379895.11687

selectivity, and amazing sensitivity is mostly dependent on selecting suitable working electrode materials with adequate stability and then surface-modifying them. One of the best and most efficient working electrodes for various electrosynthesis modifications is carbon paste. In order to create these electrodes, graphite powder (the conducting substance) and mineral oil (the binder) are carefully combined and ground to the ideal weight ratio. After creating a homogenous paste, it is pressed into a piston-shaped electrode holder with an electrical contact until the electrode is fully packed. Carbon paste electrodes (CPEs), composed of a blend of carbon (graphite) powder and a binding agent (pasting liquid), have emerged as a prevalent electrode material for the laboratory fabrication of diverse electrodes, sensors, and detectors. Compared to analogous PVC and coated wire electrodes, CPEs exhibit much lower Ohmic resistance, rapid reaction times, simplicity of production and regeneration, as well as extended functional longevity [20-22]. The handmade carbon paste, composed of carbon powder and a liquid binder, was pliable, lacked appropriate materials, and required containment within a specialized electrode holder [20-22]. The synthesis of Mn(II)-imprinted polymer contributes to a specific recognition mechanism, which would suggest tha t when combined with a carbon paste electrode (CPE), the enhanced selectivity would be reflected in the overall affinity of the electrode for Mn(II) ions, and the work hereby demonstrates that this is the case. The template polymer has selective cavities, which enables exceptional selectivity for Mn(II) while limiting the interference of the competing cations. In complex sample matrices (like the petroleum water), many metal ions may interact, making this selectivity critical. [20-22].

With the use of ion-imprinted polymer (IIP) technology, a particular metal ion can be selectively extracted and recovered. Furthermore, template ions can be easily removed from polymeric particles via leaching by mineral acid; then the created cavities have the same size and shape as the metal ion that was imprinted [23].

Carbon nanotubes (CNTs) were also comprised in the fabrication of carbon paste electrodes [24-26], wherein the carbon nanotubes are characterized by considerable thermal conductivity, significant specific surface area, and superior electrical properties [27, 28].

The article presents the development of a novel Mn(II) ion-selective electrode (ISE) based on carbon paste, incorporating a manganese ion-imprinted polymer as the ionophore (Scheme 1). The molecularly imprinted polymer (MIP) was synthesized via the polymerization of ethylene glycol dimethacrylate (EGDMA) and methacrylic acid (MAA), followed by characterization through various analytical and spectroscopic techniques. When compared to other kinds of ion-selective electrodes (ISEs), Mn(II)-ISEs have unique benefits and drawbacks. In general, ISEs work by using a selective membrane to detect particular ions in a solution and producing an electrical potential that is proportionate to the ion concentration. The newly developed ISEs demonstrated a broad concentration range, rapid response time, and high reproducibility. High selectivity for Mn(II) ions is provided by Mn(II) ISEs, especially those that use molecularly imprinted polymers (MIPs), which reduce interference from other cations. Compared to traditional ISEs, which could have cross-sensitivity to comparable ions, this is a major benefit. Furthermore, Mn(II) ISEs have broad concentration ranges and quick reaction times, which makes them useful for real-time monitoring in complicated samples like petroleum water. Furthermore, precision and accuracy parameters—including inter- and intraday detection and quantification, standard deviation, relative standard deviation, percentage recovery, and comprehensive validation metrics—were systematically evaluated and reported.

2. Experimental

2.1. Materials

Analytical-grade commercial reagents were utilized in this investigation, and deionized water was used for all experimentation. Manganese chloride ($MnCl_2.4H_2O$), ammonium hydroxide, graphite powder (synthetic 1–2 µm), and tricresylphosphate (TCP) have been obtained through Sigma-Aldrich. Hopkin and Williams provided diphenylthiocarbazone (dithizone). Ethylene glycol dimethacrylate (EGDMA), ammonium persulfate, and isopropanol were acquired from Merck.

The following chemicals were utilized for making carbon paste electrodes (CPEs): dioctylphthalate (DOP), dibutylphthalate (DBP), dioctylsebacate (DOS), and hydrochloric acid were supplied from BDH, while *o*-nitrophenyloctylether (*o*-NPOE) was supplied from Fluka. Highly pure multi-walled carbon nanotubes (MWCNTs) (diameter within 10–20 nm) were purchased from the Egyptian Petroleum Research Institute.

2.2. Apparatus

A Jenway 3505 pH meter was used to measure potential. A silver-silver chloride double-junction reference electrode was used in conjunction with several ion-selective electrodes (Metrohm 6.0726.100). Thermo-Orion, model Orion 3 stars, USA, was used to measure pH. Before being analyzed, every piece of glassware used in this study was thoroughly cleaned and allowed to dry in an oven. The Scanning Electron Microscope (SEM) for Mn(II)-IIP via SEM Model Quanta 250 FEG (Field Emission Gun) is attached with EDX Unit (Energy Dispersive X-ray Analyses), with accelerating voltage 30 K.V., magnification 14 × up to 1000000, and resolution for Gun.1n (FEI company, Netherlands). The Fourier-transform infrared spectroscopy (FTIR) spectra were recorded on [Model] Thermo Scientific Nicolet iS10 spectrometer (4000–400 cm^{-1}) in KBr/Ge mid infrared optimized. [Company] Thermo Fisher Scientific, USA and a room temperature deuterated triglycine sulfate (DTGS) detector was used for the analysis, System Software verification (SPV) software (Thermo Scientific OMNIC^{TM} software) was used. They were measured at the Egyptian Petroleum Research Institute.

2.3. Samples

In this investigation, water samples were sourced from three diverse locations to assess their properties. The first sample, referred to as formation water (sample 1), was collected from the Khalda Petroleum Company situated in Kalabsha within the Western Desert region. The second sample, designated as river water (sample 2), was obtained from Garden City, a central district in Cairo, Egypt. The third sample, identified as seawater (sample 3), was gathered from Ras Ghareb along the Red Sea coastline of Egypt. This selection of samples facilitated a comprehensive evaluation of water from distinct environmental contexts.

2.4. Synthesis of Manganese Ion Imprinted Polymer

Thermal polymerization was used to create the Mn(II)-IIP in two stages: To prepare the Mn-Dithizone complex, first dissolve 0.479 g of $MnCl_2.4H_2O$ in deionized water, then mix it with 1.0235 g of Dithizone ligand in 22.3 mL of ammonium

hydroxide. Stir the blend for about an hour, forming a brown precipitate, and then filter and dry it at 60 °C. Next, copolymerize the Mn-dithizone complex using 12.8 mmol of MAA as a monomer, 26.9 mmol of EGDMA as a cross-linker, and 0.5 mmol of ammonium persulfate as an initiator. Then, for 24 hours, the reaction temperature was kept at 60°C in an oil bath.

The resulting orange solid polymer was first dried, ground, and washed with deionized water to remove any impurities. Following polymerization, the synthesized Mn(II)-IIP particles were subjected to a leaching process by agitating them in 6 M hydrochloric acid for 12 hours to extract the Mn(II) ions. The leached precipitate was then repeatedly rinsed with deionized water until a neutral pH was achieved, indicating the effective removal of acid. This extraction resulted in a noticeable color change, with the powdered IIPs turning white upon removal of the Mn(II) ions. Finally, the white powder was dried at 60°C. The overall synthetic procedure, encompassing both the leaching and unleaching steps of the Mn(II)-IIP, is illustrated in Scheme 1.

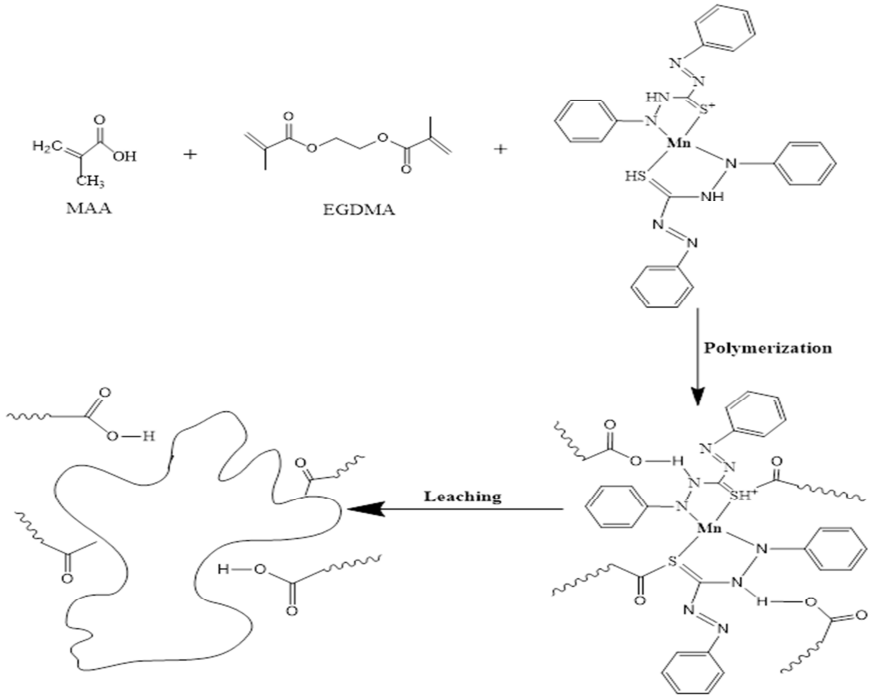

Scheme 1: Schematic illustration of the process used to create Mn(II)-Ion Imprinted Polymer.

2.5. Fabrication of carbon paste electrodes (CPEs)

In a mortar, 250 mg of pure graphite powder is thoroughly blended with 7–17 mg of the Mn(II)-MIPs ionophore in the presence of a plasticizer. Specifically, 0.125 mL of one of the following plasticizers—DOS, DOP, TCP, o-NPOE, or DBP—is added during the mixing process. This modified paste is subsequently used to fill the electrode body, which is then immersed in distilled water for 24 hours before use [29-31]. After the immersion period, the carbon paste surface is carefully polished with filter paper by gradually advancing a stainless-steel screw, thereby exposing a new, smooth electrode surface.

2.6. Equilibration of electrode and potential measurements

At ambient conditions, the electrode potential was systematically measured by incrementally increasing the concentration of Mn(II) ions in the test solution, spanning a range from 1.0×10^{-7} to 1.0×10^{-1} mol L^{-1}, while maintaining continuous stirring to ensure homogeneity. Measurements were recorded once the potential stabilized within a tolerance of 0.1 mV, signifying that equilibrium had been achieved.

Subsequently, calibration graphs were constructed by plotting the stabilized electrode potential values as a function of the logarithm of Mn(II) ion concentration (log [Mn(II)]). These calibration curves served as the basis for quantifying the manganese content in various water samples analyzed in this study. The method allowed for precise determination of unidentified Mn(II) concentrations by comparing the measured potentials against the established calibration trend.

2.7. Water samples preparation

Water samples from multiple locations, as outlined in the experimental section, were analyzed to determine their manganese (II) ion content. Prior to analysis, all samples underwent filtration to eliminate particulate matter that could compromise the accuracy of the measurements. The filtered samples were then subjected to analysis using the modified carbon paste electrode in combination with the direct calibration method. This approach allowed for precise and reliable quantification of Mn(II) levels, thereby validating the sensor's effectiveness and suitability for environmental monitoring applications.

2.8. The Matched Potential Method (MPM)-selectivity coefficients

Two experiments are used to determine the matched potential selectivity coefficient. The potential change that occurs when the concentration of primary ions in the reference solution is altered is first measured. The authors' example suggests that the possible shift in this step should be between 10 and 30 mV. As in the first experiment, "an identical reference solution would be mixed with an interfering ion until the same potential change is obtained" in the second experiment. The ratio of the concentration of interfering ions after the second experiment to the rise in the concentration of primary ions in the first would be the selectivity coefficient.

3. Results and discussion

We delineated the metal-sensitive electrodes using liquid or polyvinyl chloride (PVC) membranes. Drawbacks in the usage of polyvinyl chloride membrane electrodes have arisen from the time-consuming and inconsistent hand manufacturing processes, the difficulty of fabricating them in tiny sizes, and the shorter lifetime of the electrode. CPEs offer various benefits, including extremely low Ohmic resistance, cheap cost, reaction time, repeatability of the preparation process, and a cheap and rapid preparation procedure. This allows the potential of measurements on tiny amounts as well as capabilities for the design of a portable titration device for field titration of metals [19, 21]. Therefore, the purpose of this paper is the fabrication of a unique modified carbon paste electrode for the measurement of Mn(II) in pure and diverse water samples. The novel electrode was extensively described following ICH principles.

3.1. Characterization of polymers

Fourier-transform infrared spectroscopy (FTIR) spectra of unleached and leached ion-imprinted polymers (IIP) were recorded as being illustrated in Fig. 1, which demonstrates that both polymeric materials have nearly identical polymeric backbones, which indicates that the leaching process with a strong acidic solution didn't affect the chemical stability of the ligand in the polymer matrix [32, 33].

The FTIR spectra of the Mn-ion imprinted polymer (Mn-IIP) before (unleached) and after (leached) Mn removal reveal distinct changes that confirm successful template extraction and formation of specific recognition sites. In the unleached Mn-IIP spectrum, prominent absorption peaks are observed at 2993.6, 1727.9, 1631.5, 1461, 1389.9, 1253.9, and 1164.8 cm^{-1}. The peak at 2993.6 cm^{-1} is attributed to C–H stretching vibrations from aliphatic chains in the polymer backbone. The strong band at 1727.9 cm^{-1} corresponds to the ester carbonyl (C=O) stretching of MAA and the cross-linker EGDMA, confirming successful polymerization. The 1631.5 cm^{-1} peak is characteristic of C=N stretching from the dithizone ligand coordinated to Mn(II), while the peaks at 1461 and 1389.9 cm^{-1} are assigned to C–H bending and C–N stretching, respectively. The bands at 1253.9 and 1164.8 cm^{-1} are indicative of C–O and C–S stretching vibrations, reflecting the presence of the dithizone moiety within the polymer matrix. After leaching, the FTIR spectrum demonstrates several notable changes. The C–H stretching band shifts to 2929.12 cm^{-1}, and the carbonyl peak appears at 1724.9 cm^{-1}, maintaining its intensity and confirming the structural stability of the polymer backbone. The C=N and aromatic-related region at 1631.5 cm^{-1} in the leached sample has disappeared, followed by a diminished peak at 1458.75 cm^{-1}, indicating the disruption of the Mn-IIP and the removal of Mn(II) ions. The C–N and C–S associated bands shift to 1393.9 and 1268.6 cm^{-1}, respectively, and show reduced intensity, further supporting the transition from coordinated to free dithizone sites. Additionally, the transformation of the 1161.8 cm^{-1} band—its diminished intensity and splitting into two broad peaks after leaching (at 1161.8 and 1115.3 cm^{-1}) provides compelling molecular evidence for the successful imprinting and activation of selective recognition sites in the Mn-IIP. This observation, alongside the stability of the main polymer backbone (as evidenced by the unaltered carbonyl region), underscores the effectiveness of the imprinting strategy and the readiness of the material for targeted Mn(II) adsorption in environmental or analytical applications (Fig. 1) [32].

Overall, the diminished intensities and subtle shifts of key peaks after leaching provide compelling evidence for the successful removal of Mn(II) ions and the generation of specific recognition sites within the Mn-IIP. The preservation of the carbonyl band and the emergence of new features in the fingerprint region highlight the robustness of the polymer network and the creation of functionalized cavities, which are essential for selective Mn(II) adsorption in subsequent applications (Fig. 1).

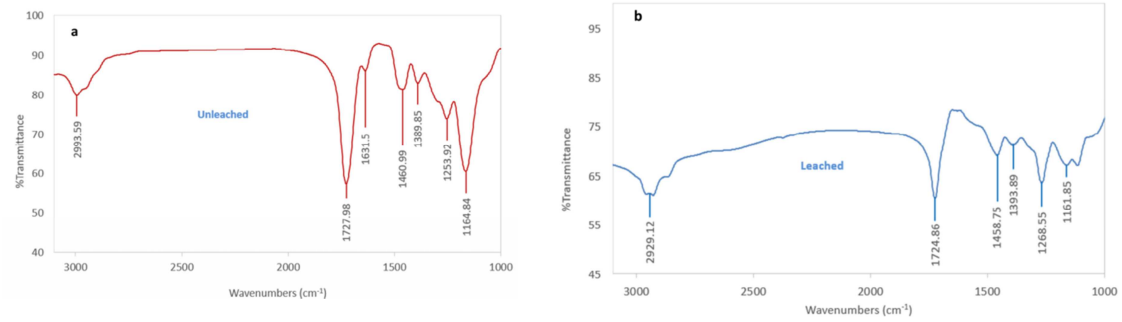

Fig.1: FT-IR spectra of (a) unleached and (b) leached Mn (II)-IIP.

3.2. SEM and EDX analyses of the fabricated carbon paste electrode

The selective extraction of the target ion with the help of a plasticizer is what determines how well a modified carbon paste electrode works. SEM and EDX techniques were utilized to verify its stability.The surface morphology of the sensor (III) was depicted using energy dispersive X-ray analysis (EDX) (Fig. 3) and scanning electron microscopy

(SEM) (Fig. 2) in an effort to correlate the potentiometric response to surface morphology. Following preparation in accordance with its ideal composition, the suggested sensor (III) was immersed for one hour in 1.0×10^{-3} mol L^{-1} of manganese ion solution. The development of illuminated spots filling the cavities between these carbon grains and the change in surface morphology after soaking demonstrate that the sensor surface is homogeneous, permeable, and contains grains that spur diffusion of Mn(II) ions. These changes can be explained by the complex formation between the Mn(II) ions and the used modifier. EDX spectrum of the carbon paste electrode (III) prior to soaking in manganese ion solution confirms the complete removal of manganese ion from the polymer matrix. Additionally, EDX spectrum after soaking in manganese ion solution emphasizes the ability of the carbon paste electrode (III) to hold manganese ion in solution, as illustrated in Fig. 3.

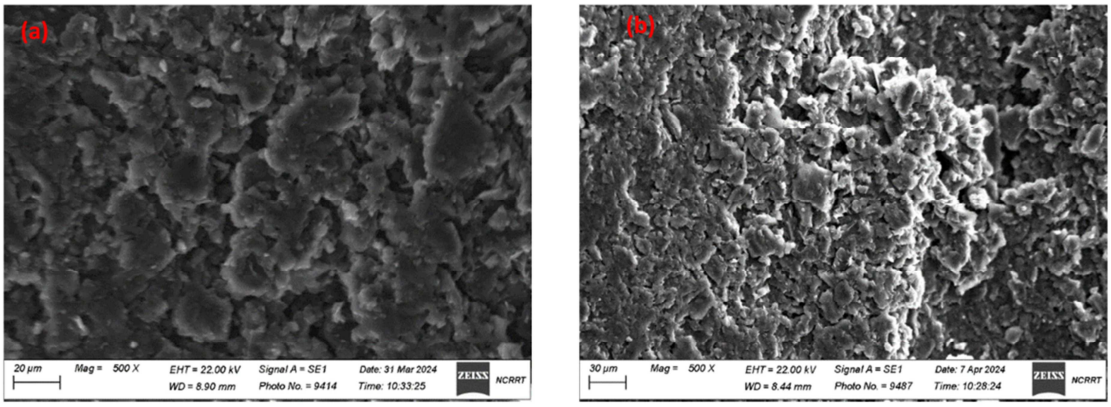

Fig. 2: SEM image of the proposed electrode (III) surface (a) before and (b) after soaking in 1.0×10^{-3} mol L^{-1} Mn(II) ion solution for an hour at 25 °C.

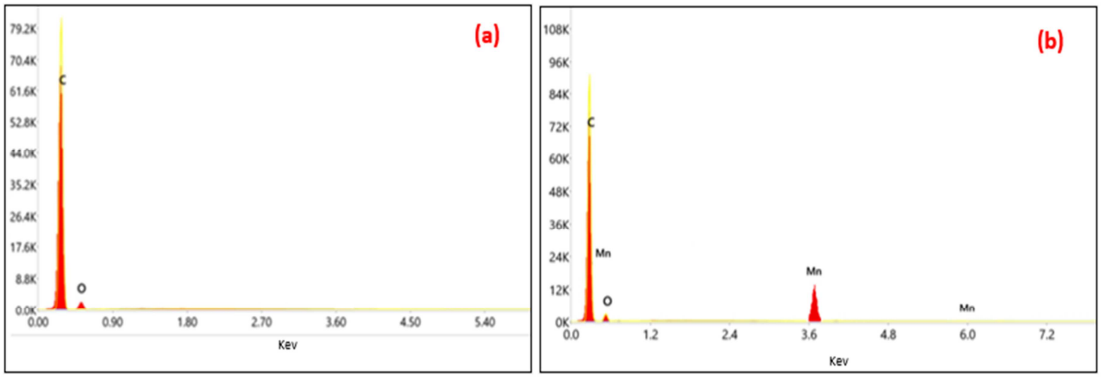

Fig. 3: EDX spectra for the proposed electrode (III) (a) before and (b) after soaking in 1.0×10^{-3} mol L^{-1} Mn(II) ion solution for an hour at 25 °C

3.2. Effect of Ionophore Contents

For potentiometric sensors or ion-selective electrodes, ionophores impeded in the sensing composition of the electrode mainly affect the sensitivity and selectivity of the electrode towards Mn(II) ions [34-45]. The ionophore (or ion carrier) is the most essential sensing component of an ion-selective electrode. It preferentially binds the target ion while discriminating against interfering ions [34-45]. To accomplish this goal, five modified CPEs were created with 7, 9.5, 12, 14.5, and 17 mg of Mn(II)-MIP ionophore; all other components were left unaltered**.** The potential of the modified CPEs made with different ionophore pastes was measured, and results are demonstrated in Fig. 4. Each electrode underwent potentiometric calibration, and the Nernstian slopes that resulted were determined to be 25.74, 26.94, 29.74, 29.05, and 28.48 mV $decade^{-1}$, respectively. These data clearly show that the 12 mg Mn (II) MIP (29.74 mV $decade^{-1}$) (electrode III) ionophore produced the best Nernstian slope (Fig. 4). The electrode surface was replaced prior to performing a fresh round of measurements in order to obtain the best analytical parameters**.** When Mn(II) concentration reduced from greater to lesser levels, residual manganese ions on the electrode surface produced the lowest linearity ranges and detection limits. This is due to adsorption of the electrodes' surface to metal cations from the sample solution [41-45].

It should be noted that the addition of a lipophilic anion increased the selectivity, response behavior, and ohmic resistance of cation-selective electrodes while also increasing their sensitivity in instances where extraction is poor [31-32].

The CPE (electrode III) was produced using o-NPOE as a plasticizer. The potential response of modified carbon paste

electrodes (III) for the detection of Mn(II) solutions was investigated. The electrodes had a linear response in the concentration range of 1.0×10^{-7} -1×10^{-1} mol L^{-1} with a Nernstian slope of 29.74 ± 0.18 mV $decade^{-1}$. The limit of detection (LOD) is found to be 1.0×10^{-7} mol L^{-1}. The results of these measurements were used to calculate the MCPE's analytical characteristics, which include the working concentration range, limit of detection, response time, and slope of the linear part of the response curve. Table 3 summarizes these parameters [41-45].

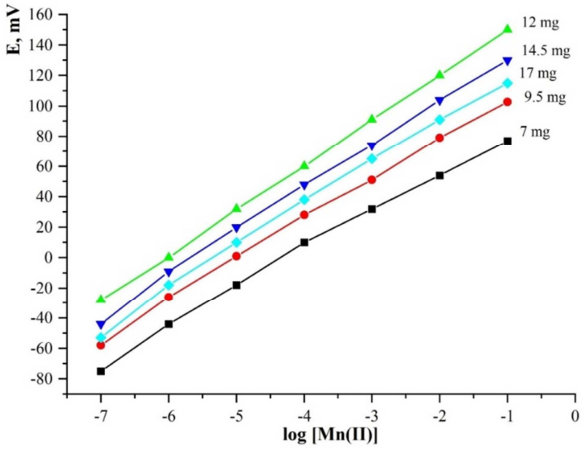

Fig. 4: Ionophore content effect on Mn(II)–carbon paste electrode.

3.3. Plasticizer effect

Plasticizer plays an important role in the electrode's sensitivity, selectivity, detection limit, and electro-active cation mobility [46]. The plasticizer used in a sensing electrode can influence the mobility of the ionophore molecules and hence have a great effect on the potential response characteristics [35]. A good plasticizer should have a low tendency of exudation from the matrix, a high capacity to dissolve other additives in the electrode, and an adequate dielectric constant [35]. Investigations were conducted on the effects of various polarities of some plasticizers comprising DOS, DOP, DBP, TCP, and *o*-NPOE on the properties of modified carbon paste electrodes under study. The potential of the modified CPEs made using various plasticizers was measured, and results are demonstrated in Fig. 5. Each electrode underwent potentiometric calibration, and the Nernstian slopes that resulted were determined to be 28.5, 27.9, 27.01, 29.17, and 29.74 mV $decade^{-1}$, respectively [38-42].

As illustrated in Fig. 5, the electrode that contained *o*-NPOE plasticizer typically exhibited superior potentiometric responses in terms of linearity range and sensitivity, and the Nernstian slope was 29.74 mV $decade^{-1}$. The results of Fig. 5 demonstrate that *o*-NPOE is a superior plasticizer, and 12 mg was the ideal ionophore content. This suggests that the plasticized paste using *o*-NPOE modifies the mobility of ion exchanger sites as well as the paste permittivity, producing the best selectivity and sensitivity feasible. Mn(II) was measured using this electrode in both pure and actual spiked water samples [38-42].

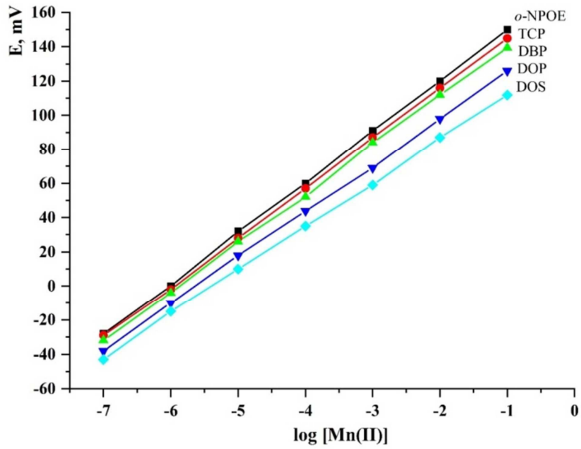

Fig. 5: Plasticizer effect on performance of Mn(II)–carbon paste electrode.

3.4. Lifetime

As per the recommendation of IUPAC, the lifespan of a sensor was studied and ascertained based on the duration between the electrode conditioning and the timing when a certain parameter of the sensor changes negatively [47]. Thereupon, a series of experiments were performed to determine the period of time during which the gained measurement results remain without any notable change. It is worth mentioning that no significant change in Nernstian slopes (29.74 ± 0.93 mV $decade^{-1}$) was observed for the proposed electrode (III) during the time frame ranging from a

day to 125 days. The proposed electrode (III) is durable and could be used for four months without any measurable drift. As illustrated in Fig. 6, over an extended period of time, the paste electrode's response stayed essentially constant.
This might be explained by a fall in plasticizer and ionophore levels in the paste due to migration. As a result, the slope value, working concentration range, and detection limit of Mn(II)-IIP may be maintained for three to four months with no detectable change [30-32].

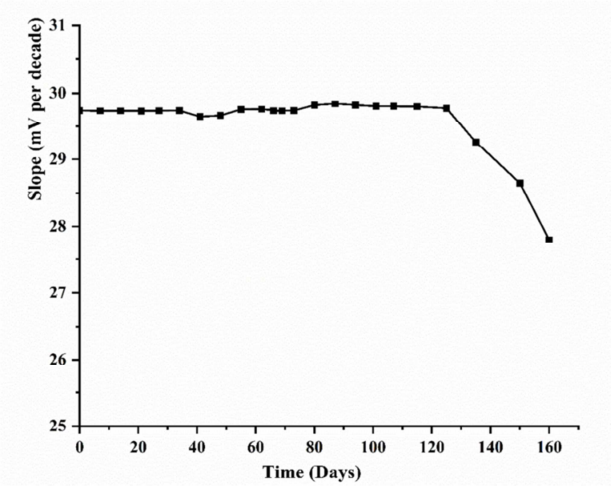

Fig. 6: Lifetime of Mn (II)–carbon paste electrode (III).

3.5. Response time

Temperature at which the test was conducted, along with other factors such as stirring, ionic concentration, and test solution composition, can all affect a sensor's response time [48]. One way to investigate the electrode's practical response time was to change the concentration of Mn(II) ions from 1.0×10^{-7} to 1.0×10^{-1} mol L^{-1}. The results presented in Fig. 7 make it evident that the suggested electrode has a response time of 8 s. This phenomenon is likely due to the rapid exchange kinetics involved in the adsorption and desorption of Mn(II) ions with ionophore in the interface between the paste and tested solution [40-43].

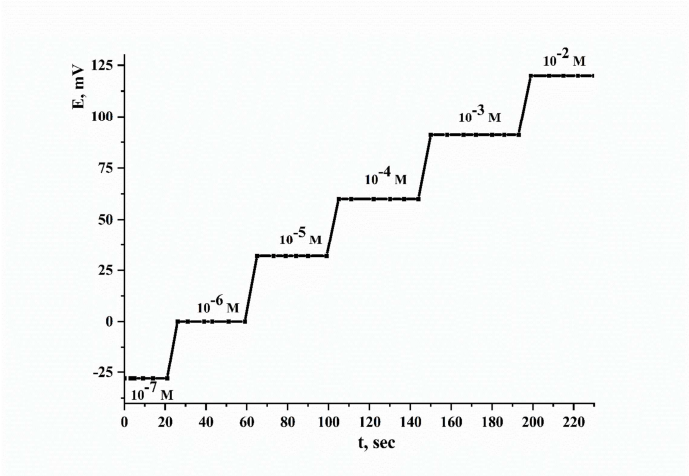

Fig. 7: The dynamic response time of electrode (III) gained by a consecutive increment in Mn(II) ion concentration.

3.6. pH effect

Studying the pH influence of the tested solutions on the potentiometric response at different concentrations of Mn(II), at 1.0×10^{-5} and 1.0×10^{-3} mol L^{-1}. Changes in acidity and basicity were carried out through adding trace amounts of hydrochloric acid and/or sodium hydroxide to the medium. At certain values of pH, potential readings were traced and recorded. The gained potential readings were graphically illustrated in Fig. 8. It was found that the potential readings remain unchanged at pH ranges from 3.5 to 8.5. The gained results indicate that there was a significant deviation in the potential readings at both low and high pH values. Specifically, at pH less than 3.5, hydronium ion interference may occur, leading to high potential readings; conversely, at pH greater than 8.5, sodium hydroxide may precipitate Mn (II) hydroxide, resulting in low potential readings [32-37].

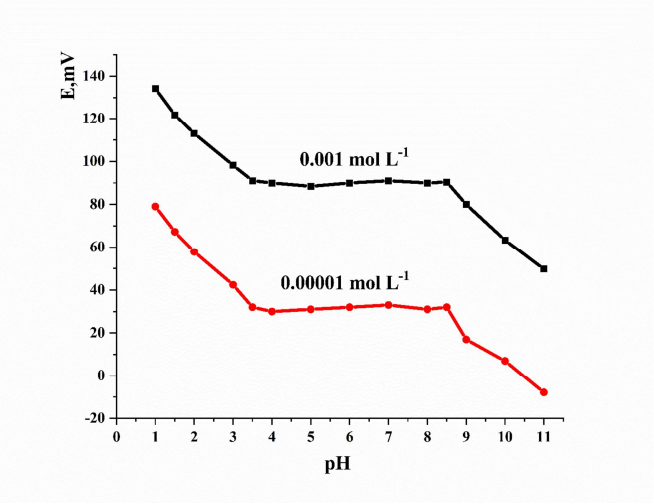

Fig. 8: pH effect on the performance of electrode (III).

3.7. Temperature effect

Investigating the impact of temperature on the fabricated electrode's response, wherein the potential of Mn(II) solutions (1.0×10^{-7} to 1.0×10^{-1} mol L^{-1}) was determined in a temperature range (10-60°C) through graphing the standard electrode potential (E°cell.) at various temperatures against (t-25), where (t) is the experiment's temperature in degrees Celsius. At p[Mn(II)] = 0, the intercepts were used to obtain the standard electrode potentials (E°). Antropov's equation indicates that a straight-line plot is produced [48, 49]:

$$E^{\circ} = E^{\circ}_{(25)} + (dE^{\circ}/dt)(t-25)$$

Where $E^{o}(25)$ is defined as the standard electrode potential at 25°C. The isothermal temperature coefficient of the proposed electrode (III) was gained from the slope of the straight-line representation. According to the results presented in Fig. 9, the isothermal coefficient was found to be 0.00016 V/°C. Consequently, the proposed electrode (III) has thermal stability up to the operational temperature of 60°C and without any observable drift in Nernstian behavior [50, 51], but at higher temperatures than 60°C, there was a significant deviation in Nernstian behavior, and this is due to damages caused by leaching of the paste matrix in the electrode surface, which results in lowering the electrode response [52].

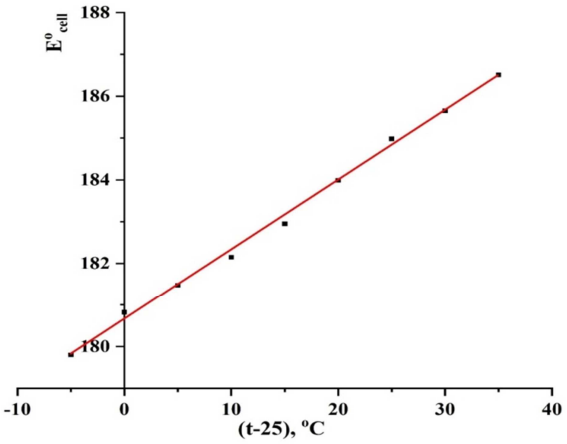

Fig. 9: Temperature effect on the performance of electrode (III).

3.8. Potentiometric selectivity

The selectivity coefficient, $K^{pot}_{A,B}$, is a significant factor for any ion-selective electrode, wherein the obtained potential values measure the targeted ion's relative response when other ions are present in the test solution. The matched potential technique (MPM) was applied for determining selectivity coefficients [48, 52, 53]. Accordingly, a fixed concentration of Mn(II) (1.0×10^{-3} mol L^{-1}) at pH 4.0 and various quantities of interfering ions have been added, then selectivity coefficients determined as per the equation hereunder:

$$K^{pot}_{A,B} = \frac{\Delta a_A}{a_B} = \frac{a'_A - a_A}{a_B}$$

Measuring values of potential change When the activity of the targeted ion a_A increases to a'_A, then the interfering ion of activity a_B is added to the targeted ion solution of activity a_A, and the same shift in potential takes place. $K^{pot}_{A,B}$ is then

calculated.

Selectivity coefficient values for the proposed electrode (III) are listed in Table 1. Possible interferences from a variety of cations and anions were investigated, and the findings are presented in Table 1. Table 1 shows that the majority of the selectivity coefficients are very low, indicating that there is no substantial interference in the electrode's performance in determining Mn(II) ions [48-50].

Table 1: Selectivity coefficients of various ions via utilizing the proposed electrode (III)

Interfering ions	$-log\ K^{MPM}_{A,B}$
Ag^{+}	5.34
Na^{+}	5.02
K^{+}	5.87
Li^{+}	6.63
Ba^{2+}	3.43
Cd^{2+}	3.78
Sr^{2+}	4.32
Pb^{2+}	4.56
Zn^{2+}	3.15
Mg^{2+}	3.89
Cu^{2+}	2.18
Al^{3+}	305
Fe^{3+}	1.93
Cl^{-}	4.03
I^{-}	4.15
Br^{-}	3.97

3.9. Analytical applications

Three actual spiked water samples were used to measure the Mn(II) concentration. Adjusting the pH of tested solutions through adding NaOH and HNO_3. The proposed potentiometric electrode was used to measure the Mn(II) ion content from the calibration graphs after the tested water samples were spiked with a specific concentration in accordance with the experimental section. Measurements gained from the potentiometric calibration are detailed in Table 2, and then these measurements were contrasted with the measurements gained from atomic absorption spectrometry (AAS), which indicate that the proposed portable modified carbon paste electrode in this investigation can be utilized for analysis of Mn(II) ion in onsite samples, as well as without any necessity for sampling in order to conduct laboratory analysis [53].

Table 2: Determination of Mn (II) in real spiked water samples via utilizing the proposed electrode (III)

Sample No.	[Mn (II)] $mgmL^{-1}$						
	Added	Found	R.S.D (%)	Recovery (%)	AAS	R.S.D (%)	Recovery (%)
1	0.35	0.345	0.837	98.57	0.341	1.773	97.43
	0.5	0.492	0.961	98.40	0.489	1.599	97.80
2	0.65	0.647	1.021	99.54	0.638	1.479	98.15
	0.7	0.693	0.995	99.0	0.688	1.384	98.29
3	0.55	0.546	1.145	99.27	0.541	1.073	98.36
	0.6	0.594	1.098	99.0	0.590	1.312	98.33

3.10. Comparative study

Data gained and revealed in Table 3 demonstrates a comparison between several manganese selective electrodes and the data of the proposed modified electrode regarding response time, working pH, slope, linear range, and detection limit [53-62]. It is worth mentioning that the electrode is superior compared to the previously reported electrodes. Such a

proposed carbon paste electrode is cheap, very simple, and durable, and with improved sensitivity and selectivity to Mn(II) ions from a broad range of other heavy metal ions, it is practically possible to use it in a wider concentration range, especially in industrial sampling, with a fast response and, to some extent, a long lifespan.

Table 3: Benchmarking between the proposed electrode (III) and several published electrodes previously.

References	Slope (mV decade^{-1})	Response time (sec)	pH	Lifetime (months)	Linear range (mol L^{-1})	DL (mol L^{-1})
[53]	30.04	5	3.0 – 9.0	4	2.7×10^{-8} – 1.0×10^{-1}	2.7×10^{-8}
[54]	29.5±0.4	9	3.5 – 9.0	4	1.2×10^{-8} – 1.0×10^{-1}	4.78×10^{-9}
[55]	29	11	4.0 – 9.5	2	6.0×10^{-6} – 2.0×10^{-2}	3.0×10^{-6}
[56]	29.3±0.5	15	4.0 – 9.0	> 2	1.0×10^{-5} – 1.0×10^{-1}	8.0×10^{-6}
[57]	29.5±0.3	12	3.0 – 9.0	3.5	4.1×10^{-7} – 1.0×10^{-1}	6.7×10^{-8}
[58]	30	10	3.0 – 6.5	2.5	5.0×10^{-6} – 1.0×10^{-1}	-
[59]	29.5	20	3.0 – 8.0	4	1.25×10^{-5} –1.0×10^{-1}	1.2×10^{-5}
[60]	30.1±1.0	10	4.5 – 7.5	-	4.0×10^{-7} –1.8×10^{-2}	1.0×10^{-7}
[61]	30.17	5	2 – 8.0	2.5	1.0×10^{-7} – 1.0×10^{-1}	1×10^{-7}
[62]	26.71±0.59	5	2.8 – 8.2	2.5	1.0×10^{-7}–1.0×10^{-1}	3.1×10^{-8}
Proposed electrode (III)	29.74	8	3.5 – 8.5	4	1.0×10^{-7} – 1.0×10^{-2}	1.0×10^{-7}

4. Conclusion

To detect Mn(II)-MIP, an electrochemical sensor with high sensitivity and selectivity was developed based on molecular imprinting techniques. The proposed electrodes displayed a Nernstian response in the working range of 1.0×10^{-7} – 1.0×10^{-1} mol L^{-1} with a detection limit of 1.0×10^{-7} mol L^{-1} and a slope of 29.74 ± 0.18 mV decade^{-1}. In the pH ranges of 3.5-8.5, it showed adequate sensitivity and stability, with rapid reaction times of 8 seconds for electrode (III). The CPE (electrode III) can be used to do routine analysis of the Mn(II) ion in pure solution and various water samples. When the response characteristics of the suggested potentiometric sensor were contrasted with those of potentiometric sensors that had already been made public, the results demonstrated that the presented sensor consistently performed better than the latter in terms of detection limits and, more importantly, selectivity over other metal ions. Mn(II) levels in different water samples can be evaluated using it. Mn(II) ions were successfully assessed using this method in a range of authentic samples, and the outcomes were consistent with those obtained using AAS.

5. References

[1] W.H. Organization, Manganese in drinking water: background document for development of WHO guidelines for drinking-water quality, World Health Organization2021.
[2] S.K. Ghosh, Diversity in the family of manganese oxides at the nanoscale: from fundamentals to applications, ACS omega, 5(2020) 25493-504.
[3] X. Zhang, A. Sathiyaseelan, K.V. Naveen, Y. Lu, M.-H. Wang, Research progress in green synthesis of manganese and manganese oxide nanoparticles in biomedical and environmental applications–A review, Chemosphere, 337(2023) 139312.
[4] M.A. Mohammed, A. Fetoh, T.A. Ali, M.M. Youssef, Y.G.A. El-Reash, G.M. Abu El-Reash, Co(II), Mn(II), and Fe(III) complexes of water-soluble hydrazone bearing 2-nicotinoylhydrazineylidene moiety: Preparation, characterization, cyclic voltammetry, computational and biological studies, Applied Organometallic Chemistry, 38(2024) e7376.
[5] J. Bi, M. Wu, Y. Liu, L. Song, L. Wang, Q. Liu, et al., Association between maternal urinary manganese concentrations and newborn telomere length: results from a birth cohort study, Ecotoxicology and Environmental Safety, 213(2021) 112037.
[6] X. Chen, G. Yang, B. Zhang, F. Li, L. Liu, F. Li, Effects of manganese-supplemented diets on growth performance, blood biochemistry, nitrogen metabolism and skeletal development of rex rabbits, Journal of Trace Elements in Medicine and Biology, 61(2020) 126543.
[7] M.R. Miah, O.M. Ijomone, C.O. Okoh, O.K. Ijomone, G.T. Akingbade, T. Ke, et al., The effects of manganese overexposure on brain health, Neurochemistry international, 135(2020) 104688.
[8] T.A. Ali, G.G. Mohamed, Synthesis and characterization of Schiff base ligand as a carrier and its application for construction of new Mn(II) sensors and their use in petroleum water samples, Egyptian Journal of Petroleum, 31(2022) 47-54.
[9] M. Jing-zhi, Condition optimization of X-ray fluorescence spectrometry with fusion sample preparation for determination of ten major and minor components in manganese ores, Analysis and Testing Technology and Instruments, 23(2017) 261-6.
[10] K. Daly, A. Fenelon, Application of energy dispersive X-ray fluorescence spectrometry to the determination of copper, manganese, zinc, and sulfur in grass (Lolium perenne) in grazed agricultural systems, Applied Spectroscopy, 72(2018) 1661-73.
[11] M.A. Ebrahim, S. Alkorashy, K. Kghodeif, A. Moemen, M.H. Shaltout, Polyaniline-intercalated manganese dioxide Nanomaterial Composites for the Removal of Fe, Al and Sr, Egyptian Journal of Chemistry, 67(2024) 169-73.

[12] Z. Cai, J. Han, J. Zhang, Determination of calcium, magnesium, aluminium, iron and manganese in wollastonite by inductively coupled plasma atomic emission spectrometry, Metallurgical Analysis, 33(2013) 45-50.
[13] A. Belozerova, A. Mayorova, N.Y. Kalinina, M. Bardina, Determination of Gallium in Nickel and Iron Alloys by Inductively Coupled Plasma Atomic Emission Spectrometry with Preseparation from the Matrix, Journal of Analytical Chemistry, 80(2025) 96-103.
[14] A.A. Gouda, Cloud point extraction, preconcentration and spectrophotometric determination of trace amount of manganese (II) in water and food samples, Spectrochimica Acta Part A: Molecular and Biomolecular Spectroscopy, 131(2014) 138-44.
[15] E.G. Moreira, D. Seo, M.B. Vasconcellos, M. Saiki, Trace element determination in a mussel reference material using short irradiation instrumental neutron activation analysis, Journal of Radioanalytical and Nuclear Chemistry, 296(2013) 251-4.
[16] Y. Liu, D. Rolle-McFarland, F. Mostafaei, Y. Zhou, Y. Li, W. Zheng, et al., In vivo neutron activation analysis of bone manganese in workers, Physiological measurement, 39(2018) 035003.
[17] L. Lesven, S.M. Skogvold, Ø. Mikkelsen, G. Billon, Determination of manganese in natural media by anodic stripping voltammetry using a rotating solid silver amalgam electrode, Electroanalysis: An International Journal Devoted to Fundamental and Practical Aspects of Electroanalysis, 21(2009) 274-9.
[18] R.D. Crapnell, C.E. Banks, Electroanalytical overview: The determination of manganese, Sensors and Actuators Reports, 4(2022) 100110.
[19] A.G.-M. Ferrari, S.J. Rowley-Neale, C.E. Banks, Screen-printed electrodes: Transitioning the laboratory in-to-the field, Talanta Open, 3(2021) 100032.
[20] B. Mostafiz, S.A. Bigdeli, K. Banan, H. Afsharara, D. Hatamabadi, P. Mousavi, et al., Molecularly imprinted polymer-carbon paste electrode (MIP-CPE)-based sensors for the sensitive detection of organic and inorganic environmental pollutants: A review, Trends in Environmental Analytical Chemistry, 32(2021) e00144.
[21] T. Awad Ali, A.A. Abd-Elaal, G.G. Mohamed, Screen printed ion selective electrodes based on self-assembled thiol surfactant-gold-nanoparticles for determination of Cu(II) in different water samples, Microchemical Journal, 160(2021) 105693.
[22] M. Roushani, Z. Saedi, F. Hamdi, B.Z. Dizajdizi, Preparation an electrochemical sensor for detection of manganese (II) ions using glassy carbon electrode modified with multi walled carbon nanotube-chitosan-ionic liquid nanocomposite decorated with ion imprinted polymer, Journal of Electroanalytical Chemistry, 804(2017) 1-6.
[23] P.E. Hande, A.B. Samui, P.S. Kulkarni, Highly selective monitoring of metals by using ion-imprinted polymers, Environmental Science and Pollution Research, 22(2015) 7375-404.
[24] S.J. Malode, P. Sharma, M.R. Hasan, N.P. Shetti, R.J. Mascarenhas, Carbon and carbon paste electrodes, Electrochemical Sensors, Elsevier2022, pp. 79-114.
[25] S. Tajik, H. Beitollahi, F.G. Nejad, M. Safaei, K. Zhang, Q. Van Le, et al., Developments and applications of nanomaterial-based carbon paste electrodes, RSC advances, 10(2020) 21561-81.
[26] S. Tajik, M.A. Taher, H. Beitollahi, Simultaneous determination of droxidopa and carbidopa using a carbon nanotubes paste electrode, Sensors and Actuators B: Chemical, 188(2013) 923-30.
[27] M. Falk, Z. Blum, S. Shleev, Direct electron transfer based enzymatic fuel cells, Electrochimica Acta, 82(2012) 191-202.
[28] J. Chen, B. Liu, X. Gao, D. Xu, A review of the interfacial characteristics of polymer nanocomposites containing carbon nanotubes, RSC advances, 8(2018) 28048-85.
[29] T.A. Ali, G.G. Mohamed, A.H. Said, Construction and Performance Characteristics of Modified Screen Printed and Modified Carbon Paste Sensors for Selective Determination of Cu(II) Ion in Different Polluted Water Samples, Chemical Engineering Communications, 203(2016) 724-35.
[30] G.G. Mohamed, M. El-Shahat, A. Al-Sabagh, M. Migahed, T.A. Ali, Septonex–tetraphenylborate screen-printed ion selective electrode for the potentiometric determination of Septonex in pharmaceutical preparations, Analyst, 136(2011) 1488-95.
[31] T.A. Ali, G.G. Mohamed, A.H. Farag, Electroanalytical Studies on Fe (III) Ion-Selective Sensors Based on 2-methyl-6-(4-methylenecyclohex-2-en-1-yl) hept-2-en-4-one Ionophore, International Journal of Electrochemical Science, 10(2015) 564-78.
[32] N.A. Samah, N.A.M. Rosli, A.H.A. Manap, Y.F.A. Aziz, M.M. Yusoff, Synthesis & characterization of ion imprinted polymer for arsenic removal from water: a value addition to the groundwater resources, Chemical Engineering Journal, 394(2020) 124900.
[33] T.A. Ali, G.G. Mohamed, Modified screen-printed ion selective electrodes for potentiometric determination of sodium dodecylsulfate in different samples, Journal of AOAC International, 98(2015) 116-23.
[34] T.A. Ali, M. Soliman, G.G. Mohamed, A. Farag, M.K. Samah, Development of a new modified screen-printed and carbon paste electrodes for selective determination of cetyltrimethylammonium bromide in different water samples, International Journal of Electrochemical Science, 10(2015) 3192-206.
[35] R. Etefagh, E. Azhir, N. Shahtahmasebi, Synthesis of CuO nanoparticles and fabrication of nanostructural layer biosensors for detecting Aspergillus niger fungi, Scientia Iranica, 20(2013) 1055-8.
[36] T.A. Ali, G.G. Mohamed, M. Omar, V.N. Abdrabou, Improved determination of mebeverine hydrochloride in urine, serum and pharmaceutical preparations utilizing a modified carbon paste electrode, International Journal of Electrochemical Science, 10(2015) 2439-54.
[37] H. Beitollahi, S.Z. Mohammadi, M. Safaei, S. Tajik, Applications of electrochemical sensors and biosensors based on modified screen-printed electrodes: a review, Analytical Methods, 12(2020) 1547-60.
[38] T.A. Ali, A.L. Saber, G.G. Mohamed, T.M. Bawazeer, Determination of Cr (III) ions in different water samples using chromium (III)-sensor based on N-[4-(dimethylamino) benzylidene]-6-nitro-1, 3-benzothiazol-2-amine, International Journal of Electrochemical Science, 9(2014) 4932-43.

[39] E.Y. Frag, T.A. Ali, G.G. Mohamed, Y.H. Awad, Construction of different types of ion-selective electrodes. Characteristic performances and validation for direct potentiometric determination of orphenadrine citrate, Int J Electrochem Sci, 7(2012) 4443-64.
[40] G.G. Mohamed, T.A. Ali, M. El-Shahat, A. Al-Sabagh, M. Migahed, New screen-printed ion-selective electrodes for potentiometric titration of cetyltrimethylammonium bromide in different civilic media, Electroanalysis, 22(2010) 2587-99.
[41] T.A. Ali, G.G. Mohamed, E. Azzam, A.A. Abd-elaal, Thiol surfactant assembled on gold nanoparticles ion exchanger for screen-printed electrode fabrication. Potentiometric determination of Ce (III) in environmental polluted samples, Sensors and Actuators B: Chemical, 191(2014) 192-203.
[42] G.G. Mohamed, T.A. Ali, M.F. El-Shahat, M. Migahed, A. Al-Sabagh, Novel screen-printed electrode for the determination of dodecyltrimethylammonium bromide in water samples, Drug Testing and Analysis, 4(2012) 1009-13.
[43] G.G. Mohamed, T.A. Ali, M. El-Shahat, A. Al-Sabagh, M. Migahed, E. Khaled, Potentiometric determination of cetylpyridinium chloride using a new type of screen-printed ion selective electrodes, Analytica Chimica Acta, 673(2010) 79-87.
[44] O. Özbek, A. Çetin, E. Koç, Ö. Isildak, Synthesis and sensor properties of a phenol derivative molecule: potentiometric determination of silver (I) ions, Electrocatalysis, 13(2022) 486-93.
[45] T.A. Ali, G.G. Mohamed, Multi-walled carbon nanotube and nanosilica chemically modified carbon paste electrodes for the determination of mercury(II) in polluted water samples, Analytical Methods, 7(2015) 6280-9.
[46] S. Alipour, P.A. Azar, S.W. Husain, H.R. Rajabi, Synthesis, characterization and application of spherical and uniform molecularly imprinted polymeric nanobeads as efficient sorbent for selective extraction of rosmarinic acid from plant matrix, Journal of Materials Research and Technology, 12(2021) 2298-306.
[47] O. Özbek, H. Gezegen, A. Cetin, Ö. Isildak, A potentiometric sensor for the determination of Pb (II) ions in different environmental samples, ChemistrySelect, 7(2022) e202202494.
[48] T.A. Ali, G.G. Mohamed, H. Eldessouky, A.-E. Adeeb, Ion selective electrodes based on methyl 6-(hydroxymethyl) picolinate ionophore for electrochemical determination of Fe (III) in petroleum water samples, Egyptian Journal of Petroleum, 28(2019) 233-9.
[49] L. Antropov, Theoretical Electrochemistry, Mir Publisher, Moscow, Russia, (1977).
[50] C. Wardak, K. Pietrzak, M. Grabarczyk, Ionic Liquid-Multiwalled Carbon Nanotubes Nanocomposite Based All Solid State Ion-Selective Electrode for the Determination of Copper in Water Samples, Water, 13(2021) 2869.
[51] Z.F. Akl, T.A. Ali, Highly sensitive potentiometric sensors for thorium ions detection using morpholine derivative self-assembled on silver nanoparticles, RSC Advances, 6(2016) 77854-62.
[52] O. Gholipour, N. Rajabi, M.H. Razeghi, S. Arabi, A potentiometric sensor for highly selective and sensitive determination of lead(II) in industrial effluents using a synthesized metal organic framework based on zinc(II) and 4-methyl-1,2,4-triazole-3-thiol: Density functional theory and experimental studies, Microchemical Journal, 212(2025) 113496.
[53] T.A. Ali, G.G. Mohamed, Determination of Mn (II) ion by a modified carbon paste electrode based on multi-walled carbon nanotubes (MWCNTs) in different water samples, Sensors and Actuators B: Chemical, 202(2014) 699-707.
[54] M.K. Sahani, A. Singh, A. Jain, Nano-level monitoring of Mn2+ ion by fabrication of coated pyrolytic graphite electrode based on isonicotinohydrazide derivatives, Materials Science and Engineering: C, 50(2015) 124-32.
[55] I. Sheikhshoaie, T. Shamspur, S.Y. Ebrahimipur, Asymmetric Schiff base as carrier in PVC membrane electrodes for manganese (II) ions, Arabian Journal of Chemistry, 5(2012) 201-5.
[56] M. Aghaie, M. Giahi, M. Zawari, Manganese (II) ion-selective membrane electrode based on N-(2-picolinamido ethyl)-Picolinamide as neutral carrier, Bulletin of the Korean Chemical Society, 31(2010) 2980-4.
[57] A.K. Singh, K.R. Bandi, A. Upadhyay, A. Jain, A comparative study on fabrication of Mn2+ selective polymeric membrane electrode and coated graphite electrode, Materials Science and Engineering: C, 33(2013) 626-33.
[58] V.K. Gupta, A.K. Jain, G. Maheshwari, Manganese (II) selective PVC based membrane sensor using a Schiff base, Talanta, 72(2007) 49-53.
[59] A.K. Singh, P. Saxena, A. Panwar, Manganese (II)-selective PVC membrane electrode based on a pentaazamacrocyclic manganese complex, Sensors and Actuators B: Chemical, 110(2005) 377-81.
[60] M.H. Mashhadizadeh, E.P. Taheri, I. Sheikhshoaie, A novel Mn2+ PVC membrane electrode based on a recently synthesized Schiff base, Talanta, 72(2007) 1088-92.
[61] R.F. Aglan, H.H. Mahmoud, A.M. Rashad, H.M. Saleh, Novel coated wire potentiometric sensor for selective determination of Mn (II) ions in various authentic samples, Journal of the Iranian Chemical Society, 18(2021) 1567-79.
[62] M. Sanati, M. Shahinfar, M. Masrournia, H. Behmadi, Employment of Optimal Mixture Design to Optimize Selective and Sensitive Manganese (II) Potentiometric Sensor in Environmental and Biological Samples, Analytical and Bioanalytical Electrochemistry, 15(2023) 428-43.